

Cover Page



Universiteit Leiden



The handle <http://hdl.handle.net/1887/18932> holds various files of this Leiden University dissertation.

Author: Vrij, Jeroen de

Title: Improvement of oncolytic adenovirus vectors through genetic capsid modifications

Issue Date: 2012-05-10



CHAPTER 7

ENHANCED TRANSDUCTION OF CAR-NEGATIVE CELLS BY PROTEIN IX-GENE DELETED ADENOVIRUS 5 VECTORS

J de Vrij¹, SK van den Hengel¹, TG Uil¹, D Koppers-Lalic¹,
IJC Dautzenberg¹, OMJA Stassen¹, M Bárcena¹, M Yamamoto²,
CMA de Ridder³, R Kraaij³, KM Kwappenberg⁴, MW Schilham⁴
and RC Hoeben¹

¹Department of Molecular Cell Biology, Leiden University Medical Center,
Leiden, The Netherlands; ²Division of Basic and Translational Research,
Department of Surgery, University of Minnesota, Minneapolis, Minnesota, USA;
³Department of Urology, Erasmus Medical Center, Rotterdam, The Netherlands
and ⁴Department of Paediatrics, Leiden University Medical Center, Leiden,
The Netherlands

Virology 2011; 410:192-200

ABSTRACT

In human adenoviruses (HAdV), 240 copies of the 14.3-kDa minor capsid protein IX stabilize the capsid. Three N-terminal domains of protein IX form triskelions between hexon capsomers. The C-terminal domains of four protein IX monomers associate near the facet periphery. The precise biological role of protein IX remains enigmatic. Here we show that deletion of the protein IX gene from a HAdV-5 vector enhanced the reporter gene delivery 5 to 25-fold, specifically to Cocksackie and Adenovirus Receptor (CAR)-negative cell lines. Deletion of the protein IX gene also resulted in enhanced activation of peripheral blood mononuclear cells. The mechanism for the enhanced transduction is obscure. No differences in fiber loading, integrin-dependency of transduction, or factor-X binding could be established between protein IX-containing and protein IX-deficient particles. Our data suggest that protein IX can affect the cell tropism of HAdV-5, and may function to dampen the innate immune responses against HAdV particles.

INTRODUCTION

Protein IX is a non-essential protein in the capsid of human adenoviruses (HAdV). The protein has a size of 14.3 kDa, is present at 240 copies per virion, and has three highly conserved regions present in the amino (N) terminus, the central part (alanine-rich), and the carboxy (C) terminus (leucine-rich). The location and function of protein IX in the virus capsid has been the subject of investigation and debate for many years.¹ Recent work by different groups has brought consensus on its location and topology in the capsid.^{2,3} The N-terminus of the protein is located in between hexon cavities of the groups of nine (GON) hexons, presumably stabilizing the GONs. The C-terminus of the protein forms an alpha helix and is exposed on the capsid surface in close contact with hexon hypervariable region 4 (HVR4).³ C-terminal domains of three protein IX molecules associate in a parallel orientation, whereas a fourth domain binds in an antiparallel orientation.² The role of protein IX in the capsid remains enigmatic. *In vitro* analysis revealed the N-terminus of protein IX to confer a thermostable phenotype on HAdV-5 capsids.⁴ Propagation of protein IX gene deleted HAdV-5 in cell culture yields wild-type like virus titers, demonstrating that protein IX is dispensable for virus replication *in vitro*.

Protein IX has potential as an anchor for the attachment of different types of polypeptides to the viral capsid. Targeting of HAdV-5 to tumor cells has been achieved by genetically fusing protein IX to a single-chain T cell receptor directed against MHC class I in complex with MAGE-A1 peptides.⁵ Similarly, integrin-binding arginine-glycine-aspartate (RGD) peptides, as well as single-chain antibody fragments have been incorporated in this way.^{6,7} Alternatively, targeting ligands can be coupled to protein IX via the genetic inclusion of cysteine residues and subsequent chemical coupling of ligands to the reactive thiol groups.⁸ Multiple polypeptides can be incorporated simultaneously.⁹ A triple-mosaic HAdV-5 vector was developed with a poly-lysine motif, the herpes simplex virus type 1 (HSV-1) thymidine kinase, and the monomeric red fluorescent protein fused with protein IX, thereby combining targeting, therapeutic, and imaging modalities. Recently, it was demonstrated that HAdV-5 vaccine vectors with pathogen-specific antigens fused to pIX can stimulate robust protective immune responses in animals, suggesting a new route for the development of improved HAdV-5 based recombinant vaccines.^{10,11}

Here we report on the enhanced delivery of transgenes into CAR-negative cell lines as a result of protein IX-gene deletion from a HAdV-5-based vector. Furthermore, the protein IX-deficient particles demonstrated enhanced activation of peripheral blood mononuclear cells (PBMCs), and had a different *in vivo* distribution after intravenous delivery in a mouse model. The exact molecular mechanism behind this ' Δ pIX effect' remains to be delineated. Our data suggest that protein IX can affect the cell tropism of HAdV-5, and may function to dampen the innate immune responses against HAdV particles.

RESULTS

Enhanced transgene expression in CAR-negative cells with Ad5ΔE1ΔpIX

To study the role of protein IX in the HAdV-5 transduction of cells, we compared the vectors Ad5ΔE1+pIX and Ad5ΔE1ΔpIX for luciferase transgene expression in a panel of cell lines (**Fig. 1a**). Cell lines with varying expression levels of CAR were included (**Fig. 1b**). Whereas similar expression levels were obtained with both vectors in the CAR-positive cell lines HeLa, A549, and MEL2A, the vector Ad5ΔE1ΔpIX yielded higher levels than Ad5ΔE1+pIX in the CAR-negative cell lines MZ2-MEL3.0 and VH10. Since these results suggested a specific role of the protein IX lacking vector in mediating relatively higher transduction in the absence of CAR, Ad5ΔE1+pIX and Ad5ΔE1ΔpIX were analyzed for reporter gene expression in MZ2-MEL3.0 cells versus MZ2-MEL3.0/CAR cells (**Fig. 2B**). MZ2-MEL3.0/CAR cells stably expressed CAR via transduction with a recombinant lentivirus, which was confirmed by flow cytometry and immunofluorescence staining (**Fig. 2A**). In MZ2-MEL3.0 cells the reporter gene expression upon infection with Ad5ΔE1ΔpIX was found to be ten-fold increased compared to infection with Ad5ΔE1+pIX, while in MZ2-MEL3.0/CAR cells the difference was a mere two-fold (**Fig. 2b**). The enhanced transgene expression for Ad5ΔE1ΔpIX on the CAR-negative cell line MZ2-MEL3.0 appeared to be not affected by the establishment of protein IX expression in the cells (by using the recombinant lentivirus LV-CMV-pIX-IRES-NPTII¹²) prior to the transduction) (result not shown).

As a next step, the involvement of the C-terminal region of protein IX in the observed phenomenon was investigated. This domain, which is rich in leucine amino acids and is exposed on the HAdV-5 capsid as an alpha-helical structure,^{2,3} is highly conserved in human adenoviruses. The biological function of this conserved domain of protein IX is unknown. We analyzed the vector Ad5ΔE1pIX^{ΔLEU}, which lacks a major part of the C-terminal region of protein IX (amino acids 100 to 114) for reporter gene expression in MZ2-MEL3.0 and MZ2-MEL3.0/CAR. Ad5ΔE1pIX^{ΔLEU} demonstrated enhanced transduction of the CAR-negative cell line, very similar to the Ad5ΔE1ΔpIX vector (**Fig. 2c**).

To assess the appearance of the vector particles and to check for the absence of microaggregation, electron microscopy was performed on Ad5ΔE1+pIX and Ad5ΔE1ΔpIX vector batches. This showed identically shaped virus particles (**Fig. 3a**). No signs of microaggregation were observed. The Ad5ΔE1ΔpIX stock appeared to contain more small particulate matter, possibly virus debris. As previously described, pIX-deficient HAdV-5 particles have an enhanced tendency to partly dissociate into fiber- and penton base- lacking particles.¹³ However, our vectors had similar capsid incorporation levels of fiber and hexon proteins, as evident from immunoblot analyses (**Fig. 3b**), thus ruling out differences in particle dissociation for the vector preparations.

Transduction with Ad5ΔE1ΔpIX is integrin-dependent

Wild-type HAdV-5 enters cells via high affinity binding of the fiber knob domain to CAR.¹⁴ Subsequently low affinity interaction of the penton base with cellular integrins $\alpha_v\beta_3$ and $\alpha_v\beta_5$ promotes virus internalization in clathrin coated pits.^{15,16} To answer the question if Ad5ΔE1ΔpIX still uses integrins for cellular uptake, we analyzed

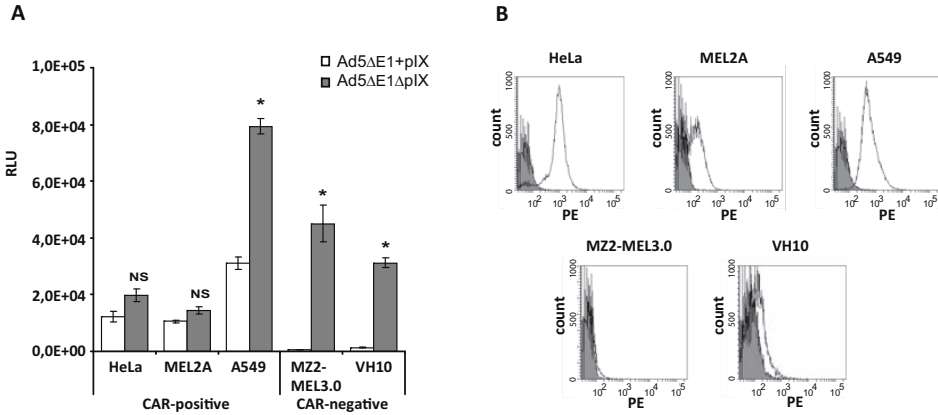


Figure 1. (a) Transduction of CAR-positive and CAR-negative cells with the replication deficient vectors Ad5ΔE1+pIX and Ad5ΔE1ΔpIX. At 24 hours post transduction (at 10 pp/cell) the luciferase expression was measured as indicated by the relative luciferase units (RLU) (NS signifies Not Significant, * $p < 0.02$ versus Ad5ΔE1+pIX). Error bars represent S.D. ($n=3$). (b) Flow cytometry with anti-CAR antibody and PE-labeled secondary antibody to analyze cell surface expression level of CAR (white histograms). The gray histograms represent incubation with secondary antibody only.

Ad5ΔE1+pIX and Ad5ΔE1ΔpIX for transgene expression (GFP) in the presence or absence of bivalent cations, which are necessary for integrin-mediated uptake of wild-type HAdV-5 into cells¹⁶ (**Fig. 4a**). This experiment again displayed a stronger reporter gene expression of Ad5ΔE1ΔpIX in MZ2-MEL3.0 cells compared to Ad5ΔE1+pIX. For both vectors the transduction appeared to be totally dependent on the presence of bivalent cations, with a complete reduction to background GFP levels for the cation-negative incubation. This is consistent with integrin-mediated uptake for both vectors. More specifically, the integrin-dependency of Ad5ΔE1ΔpIX was confirmed by a small but significant (approximately two-fold) decrease in transduction after incubation of MZ2-MEL3.0 cells with antibodies directed against $\alpha_v\beta_3$ and $\alpha_v\beta_5$ integrins (**Fig. 4b**). Similar antibody-blocking (1.5-fold reduced transduction for anti- $\alpha_v\beta_3$ and anti- $\alpha_v\beta_5$) was observed for Ad5ΔE1+pIX. Incubating the cells with higher concentrations of antibodies did not result in further reductions in transduction levels (data not shown). Anti-integrin mediated blocking of transduction was also observed on A549 cells (**Fig. 4b**). From these data we conclude that the vector Ad5ΔE1ΔpIX still uses integrins for cell internalization in CAR-deficient cells.

Reduced virus spread of the replication competent virus Ad5ΔpIX

Our data from the comparative transduction analysis suggest an alternative interaction of HAdV-5 particles lacking protein IX with the cell surface. In parallel to cell tropism extending capsid modifications described for other viruses¹⁷, it is likely that protein IX deletion from a replication competent HAdV-5 virus would result in a modified ability to spread in monolayer cell cultures. To investigate this, we constructed the replication-competent HAdV-5 viruses Ad5+pIX and Ad5ΔpIX. Both viruses expressed GFP, allowing accurate measurement of plaque size. On A549 cells the plaque size for

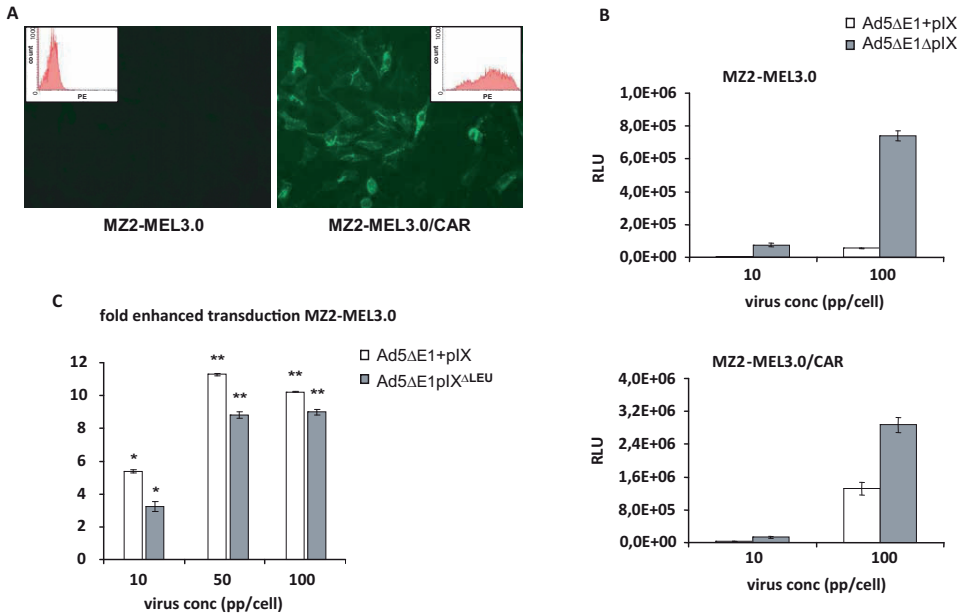


Figure 2. Transduction assays on MZ2-MEL3.0 and MZ2-MEL3.0/CAR (a) Detection of CAR expression in MZ2-MEL3.0 cells by immune-fluorescence staining with anti-CAR antibody and FITC-labeled secondary antibody. The insets represent flow cytometry histograms after staining with anti-CAR antibody and PE-labeled secondary antibody. (b) Luciferase expression in MZ2-MEL3.0 and MZ2-MEL3.0/CAR after Ad5ΔE1+pIX and Ad5ΔE1ΔpIX transduction. Error bars represent S.D. ($n=3$). (c) Fold enhancement of MZ2-MEL3.0 transduction with Ad5ΔE1ΔpIX and Ad5ΔE1ΔpIX^{ΔLEU} as compared to the transduction with Ad5ΔE1+pIX. The fold enhancements are normalized to the vector transduction ratios on MZ2-MEL3.0/CAR (* $p<0.05$, ** $p<0.005$ versus Ad5ΔE1+pIX). Errors bars represent S.D. ($n=3$).

the Ad5ΔpIX virus (median 30 arbitrary surface units (ASU), range 20-170) appeared to be significantly smaller than the plaque size for Ad5+pIX (median 100 ASU, range 30-290). A similar difference in plaque size was observed on the CAR-negative cell line VH10, with Ad5ΔpIX (median 50 ASU, range 30-150) yielding much smaller plaques compared to Ad5+pIX (median 100 ASU, range 75-280). From these analyses we conclude that protein IX-gene deletion from the genome of the replication competent virus results in a decrease in virus spread in CAR-positive (A549) as well as CAR-negative (VH10) monolayer cell cultures.

Enhanced activation of peripheral blood mononuclear cells by Ad5ΔE1ΔpIX

Our findings on the modified transduction characteristics of protein IX-deficient HAdV-5 vectors are of relevance for: (1) fundamental adeno-virology (as the findings point towards a novel biological function of protein IX), and (2) the development of protein IX-modified HAdV-5 vectors for gene therapies. For both these aspects, it will be highly interesting to determine the effect of protein IX-deletion on the interaction of HAdV-5 vectors with white blood cells. Therefore, we incubated freshly isolated

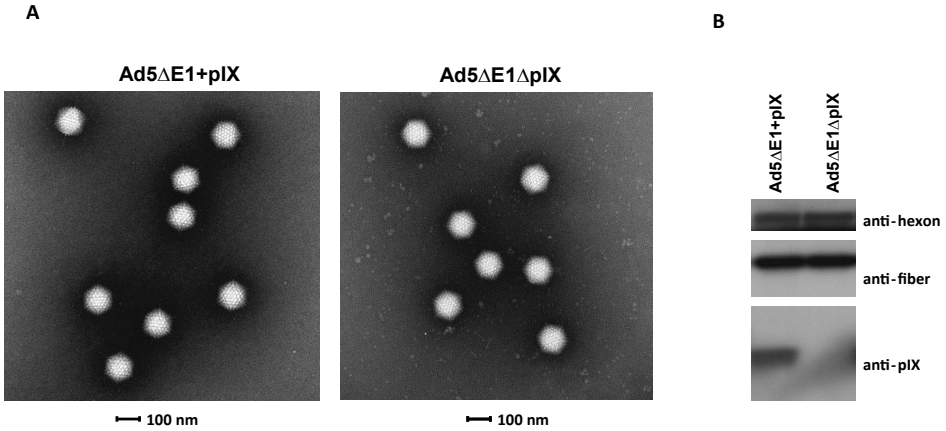


Figure 3. (a) Electron microscopy on Ad5ΔE1+pIX and Ad5ΔE1ΔpIX samples with negative staining of the vector particles in phosphotungstic acid. (b) Immunoblot detection on Ad5ΔE1+pIX and Ad5ΔE1ΔpIX lysates to analyze capsid incorporation levels of protein IX, hexon, and fiber proteins.

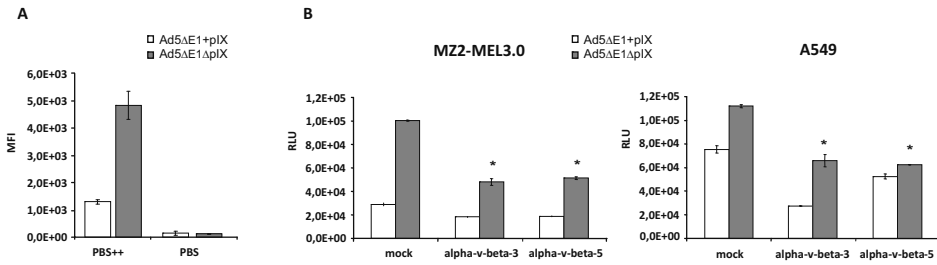


Figure 4. The effect of integrin blocking on transduction of cells with Ad5ΔE1+pIX and Ad5ΔE1ΔpIX. (a) MZ2-MEL3.0 cells were treated with EDTA to remove bivalent cations necessary for HAdV-5 interaction with integrins. Subsequent transduction was performed in the presence (PBS++) or absence (PBS) of bivalent cations and GFP expression was measured, as indicated by the mean fluorescence intensity (MFI). Error bars represent S.D. (n=3). (b) Vector mediated luciferase expression in MZ2-MEL3.0 and A549 cells in the presence or absence of antibodies directed against αVβ3 or αVβ5 integrins in the infection medium (*p<0.05 versus control treatment). Error bars represent S.D. (n=3).

human peripheral blood mononuclear cells with Ad5ΔE1+pIX and Ad5ΔE1ΔpIX, and analyzed GFP expression and the expression of cellular activation markers. This revealed relatively high levels of GFP expression in the monocyte population. The percentage of GFP-positive monocytes was similar for both vectors, varying between 10% and 30% at 100 pp/cell, depending on the donor (data not shown). For both vectors, the GFP expression in the T cell, B cell, and NK cell populations was very low (<1% GFP-positive cells). Although Ad5ΔE1+pIX and Ad5ΔE1ΔpIX showed identical GFP expression levels in the monocytes, the incubation with Ad5ΔE1ΔpIX resulted in a remarkably higher level of monocyte activation, as indicated by enhanced CD86 expression (Fig. 5a). The percentage of CD86 positive monocytes as well as the mean

fluorescence intensity for CD86 was significantly higher for the protein IX-lacking vector. This enhancement in monocyte activation was observed for monocytes derived from PBMCs of three different donors and with different virus batches. The up-regulated CD86 level involved the entire Ad5 Δ E1 Δ pIX-incubated monocyte population, not only the GFP-positive cells (**Fig. 5a**). Incubation with Ad5 Δ E1 Δ pIX also resulted in enhanced activation of NK cells, as demonstrated by an increase in CD69 expression (**Fig. 5b**). Interferon-gamma (IFN- γ) ELISA of PBMC supernatants revealed higher levels of IFN- γ production after incubation with Ad5 Δ E1 Δ pIX at the higher input virus levels (**Fig. 5c**).

Enhanced liver transduction upon intravenous administration of Ad5 Δ E1 Δ pIX

To study the functional consequences of protein IX gene deletion on biodistribution in mice, Ad5 Δ E1+pIX and Ad5 Δ E1 Δ pIX viruses were administered via tail vein injection. Luciferase expression in multiple organs was determined at 3 days post injection.

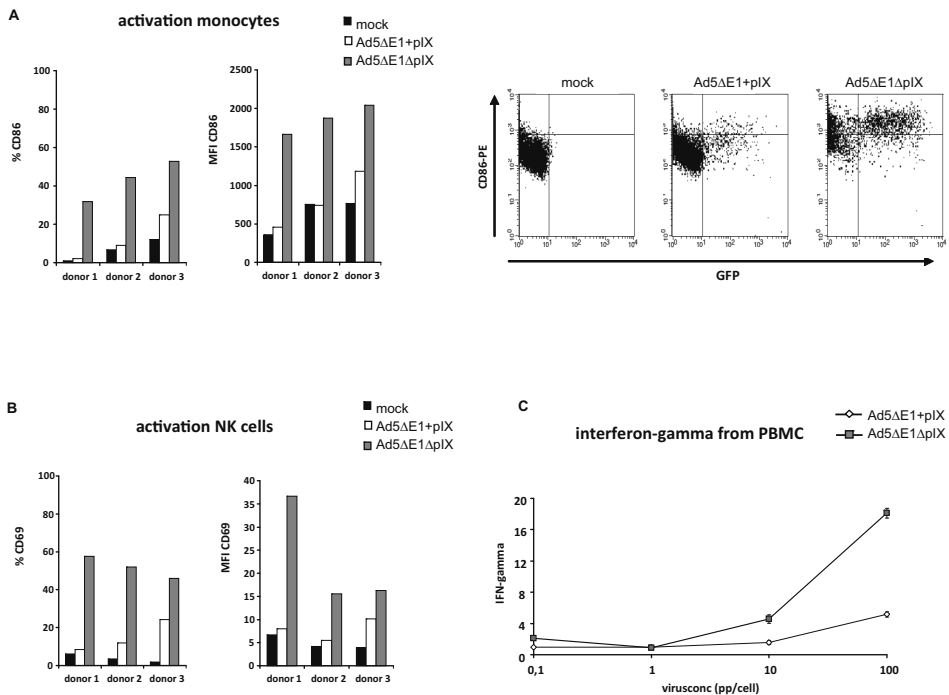


Figure 5. Activation of peripheral blood mononuclear cells (PBMCs) after incubation with Ad5 Δ E1+pIX and Ad5 Δ E1 Δ pIX for two days. **(a)** Activation of the monocyte population. The graphs on the left show the percentage of CD86 positive cells and the mean CD86 expression levels (MFI) for three different donors. The flow cytometry figures on the right illustrate the CD86 up-regulation for transduced (GFP-positive) monocytes and non-transduced (GFP-negative) monocytes (from donor 1). **(b)** Activation of the NK cell population. The percentage of CD69 positive cells and the mean CD69 expression levels (MFI) are shown for three different donors. **(c)** Measurement of IFN- γ levels in PBMC supernatant (from a single donor) after incubation with Ad5 Δ E1+pIX and Ad5 Δ E1 Δ pIX. The data represent mean values of two independent measurements.

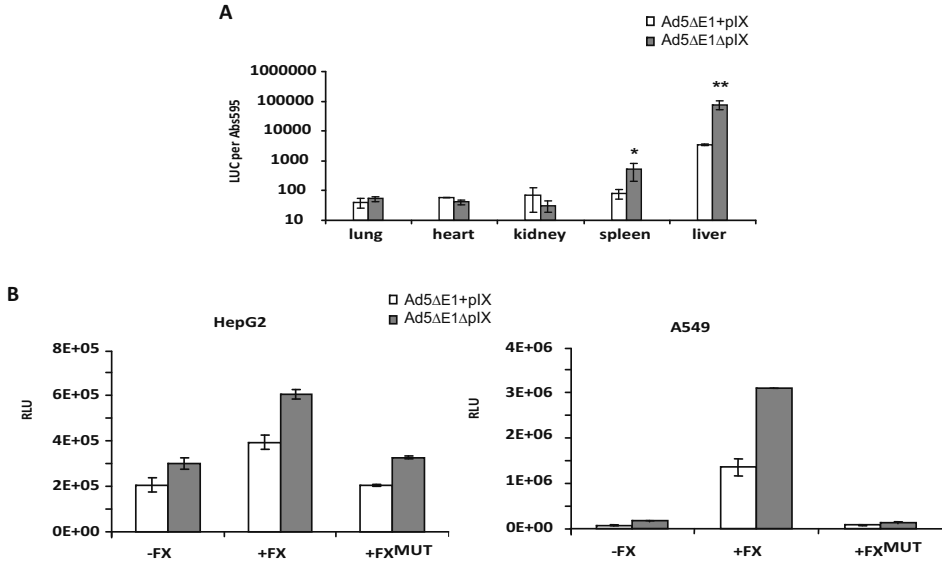


Figure 6. (a) Distribution of Ad5ΔE1+pIX and Ad5ΔE1ΔpIX in mice after tail vein injection of 10^9 vector particles. Prior to vector injection, pre-dosing was performed with the vector HAdV-5.CMV to saturate Kupffer cell macrophages. Organs were harvested three days post injection and the luciferase expression per total protein was measured (* $p=0.057$, ** $p=0.006$ versus Ad5ΔE1+pIX). Error bars represent S.D. ($n=2$). (b) Luciferase expression in HepG2 and A549 cells after transduction with Ad5ΔE1+pIX and Ad5ΔE1ΔpIX in the presence of coagulation factor X (FX), Gla-domainless mutant factor X (FX^{MUT}), or no coagulation factors (mock). Error bars represent S.D. ($n=3$).

The vector lacking protein IX yielded a more than ten-fold higher luciferase activity in the liver (**Fig. 6a**). These data show that the absence of protein IX in the viral capsid strongly affected the biodistribution of HAdV-5 particles.

Recent reports have described the involvement of plasma proteins, such as the blood coagulation factor X (FX), in HAdV-5 transduction of the liver.^{18,19} To study whether removal of protein IX influences the effects of clotting-factor binding, we compared the FX-mediated transduction for Ad5ΔE1+pIX and Ad5ΔE1ΔpIX (**Fig. 6b**). *In vitro* incubation of A549 cells and HepG2 cells with FX resulted in a similar enhancement in transduction for Ad5+pIX and Ad5ΔpIX. As expected, no effect on transduction was observed after incubation with the mutant FX (FX^{MUT}), which lacks the domain necessary for binding to the HAdV-5 capsid.¹⁹ From these data we conclude that the absence of protein IX does not affect the binding of coagulation factor X.

DISCUSSION

From our data we conclude that the omission of protein IX from HAdV-5 vectors enhances viral transduction of cell lines that are low in expression of the adenovirus receptor CAR. This finding is of relevance for the development and implementation of protein IX-gene modified HAdV-5 vectors. Also, the findings enhance our knowledge

on HAdV-5 biology and evolution, which especially becomes clear if stating our conclusion in a ‘backwards’ manner: the introduction of protein IX in HAdV-5 (making it wild-type HAdV-5) decreases viral transduction of cell lines that are low in CAR expression. Although speculative, it is very well possible that the presence of protein IX in the HAdV-5 capsid negatively interferes with non-specific cell transduction, and thereby plays a role in determining the virus tropism. Noteworthy, the extended cell tropism of the Ad5ΔE1ΔpIX vector, as presented by its enhanced transduction of CAR-negative cells, did not come with a loss in ability of CAR-mediated transduction of cells. This is clear from the comparison on MZ2-MEL3.0 and MZ2-MEL3.0/CAR. Introduction of CAR in the CAR-negative cells significantly increased transduction levels with Ad5ΔE1ΔpIX. It is conceivable that in CAR-expressing cells the protein IX-deficient particles can use either the CAR/fiber-dependent mechanism, or the CAR-independent pIX-dependent mechanism. Quantifying the relative contribution of each of these mechanisms to the total transduction requires tools for specifically blocking the new pathway. Such inhibitors remain to be identified.

Interestingly, the vector Ad5ΔE1pIX^{ALEU} had Ad5ΔE1ΔpIX-like properties, implicating the importance of the C-terminal domain of protein IX in inhibiting transgene expression in CAR-negative cell lines. The specificity for the C-terminal domain of protein IX excludes differences in viral capsid stability as a cause for the observed phenomenon, since deletion of this domain does not result in reduced capsid stability.⁴

Wild-type HAdV-5 enters cells via high affinity binding of the fiber knob domain to CAR,¹⁴ followed by interaction of the RGD motif of the penton base with cellular integrins $\alpha_v\beta_3$ and $\alpha_v\beta_5$ promoting rapid adenovirus cell entry into clathrin-coated vesicles.^{15,16} Similar to the Ad5ΔE1+pIX control virus, Ad5ΔE1ΔpIX requires the presence of bivalent cations for its transgene delivery, indicating the usage of cellular integrins for cell internalization.¹⁶ More specifically, blocking cells with anti-integrin antibodies resulted in a decrease in transduction for Ad5ΔE1ΔpIX, thereby confirming the integrin-dependency. Unfortunately, our efforts to compare the vectors for a general difference in cell binding affinity, using Alexa488-TFP (tetrafluorophenyl) labeled vector particles, were not conclusive as a result of strong and reproducible negative effects of the labeling procedure on the pIX-deficient vector particles. The effects were not identical for protein IX-positive and protein IX-negative particles, making the results obtained with these particles in comparative binding assays unreliable. Alternative protocols for fluorescent- or radio-labeling of vector particles might be more suitable for comparing the cell-binding affinity. Labeled vector particles might also be used for analysing differences in cell surface motility between protein IX-containing and protein IX-lacking vectors. Through largely unknown mechanisms HAdV-5 particles migrate on the cell surface and alterations in viral movement can result in modified transduction.²⁰

The removal of the protein IX gene from a replication competent HAdV-5 virus results in a small-plaque phenotype on CAR-positive as well as CAR-negative cell lines. This suggests the tropism modifying mutation affects the virus’s capacity to spread from cell to cell. Such small-plaque phenotypes of extended tropism mutants is not unprecedented: similar phenotypes have been described for murine corona virus mutants that acquired the capacity to bind heparin.¹⁷

To investigate the effect of protein IX-gene deletion on the interaction of HAdV-5 with human mononuclear leukocytes, we compared the vectors Ad5ΔE1+pIX and Ad5ΔE1ΔpIX for GFP expression in PBMCs. Flow cytometry analyses demonstrated GFP expression almost exclusively in monocytes, with similar expression levels for both vectors. However, increased activation of the entire monocyte population (so not exclusively restricted to the GFP-positive population) was observed for Ad5ΔE1ΔpIX, as demonstrated by an enhancement in CD86 expression. CD86 is an activation marker on antigen-presenting cells such as monocytes, macrophages, dendritic cells, and B cells, and is important for co-stimulation of T cells.²¹ The increased activation of monocytes despite similar levels of transduction (GFP expression) could be due to a direct effect on the monocytes themselves or indirectly via a more efficient stimulation of T cells or NK cells. Uptake of the protein IX-deleted vector may be increased and/or may follow different intracellular trafficking routes.^{22,23} As a consequence, more efficient viral antigen loading onto human leukocyte antigen (HLA) molecules, or an increase in CD86 expression, could lead to more T cell activation, and e.g. IFN-γ secretion. Of note, most healthy adult donors have HAdV specific T cells.²⁴ Indeed, Ad5ΔE1ΔpIX incubation resulted in enhanced production of IFN-γ. Protein IX-gene deletion appeared to affect NK cell activation as well, resulting in increased expression levels of CD69, which is an activation marker for lymphocytes including NK cells.²⁵ Increased T cell activation could have been accompanied by increased levels of other T cell cytokines like interleukin-2 (IL-2). IL-2 is a known activating cytokine of NK cells.^{26,27} Alternatively, the increased production of IFN-γ in the supernatant would also be consistent with increased activation of NK cells by the vector lacking protein IX, without the involvement of T cells.

Irrespective of the mechanism, the increased activation of monocytes and NK cells as a result of protein IX deletion is likely to have important consequences for the *in vivo* implementation of protein IX modified HAdV-5 vectors, since monocytes (after differentiation to Kupffer macrophages in the liver) as well as NK cells are important players in the sequestration of HAdV-5 vectors from the blood after systemic delivery (reviewed by Muruve²⁸). Furthermore, the observed differences in PBMC activation between Ad5ΔE1+pIX and Ad5ΔE1ΔpIX suggest a biological function of protein IX in diminishing the immune response against HAdV-5. Further studies will be necessary to fully determine the effects of protein IX deletion from HAdV-5 on the activation of immune cells.

Omission of protein IX from the capsid resulted in a remarkable difference between Ad5ΔE1+pIX and Ad5ΔE1ΔpIX upon intravenous administration in mice. Administration of Ad5ΔE1ΔpIX yielded more than ten-fold higher luciferase activity in the liver, for reasons that remain to be clarified. Extensive research has been devoted to defining the molecular mechanisms behind the sequestration of intravenously administered HAdV-5 in the human liver, with the aim to eventually improve the therapeutic efficacy of intravenously delivered HAdV-5 vectors (reviewed by Di Paolo and Shayakhmetov²⁹). The uptake of HAdV-5 in the liver has been found to occur in a CAR-independent manner and involves binding of the virus particles in the blood to complement factors and immunoglobulins (mediating uptake in Kupffer cell macrophages),^{18,30} and coagulation factors (resulting in hepatocyte transduction).^{18,19} The enhanced transduction of the liver with Ad5ΔE1ΔpIX observed in our mouse

model seems not to be a result of more efficient binding of the vector to coagulation factor X (FX), as can be concluded from our *in vitro* FX-binding assay. An alternative explanation might be that the absence of protein IX extends the HAdV-5 tropism, enabling the transduction of cells in the liver that do not present CAR. Of interest, primary human hepatocytes were recently found to have CAR localized at cellular junctions that are inaccessible to the hepatic blood flow.³¹ This localization is in contrast to the CAR molecules on hepatocellular carcinoma cells (like HepG2), being highly available for HAdV-5 binding.^{31,32}

Protein IX is strongly conserved in all primate adenoviruses indicating the importance of the protein. A biological role for protein IX in HAdV-5 capsid stabilization has been proposed, based on *in vitro* heat-stability assays.⁴ Our findings point toward other biological functions of protein IX in (i) determining the cell tropism of HAdV-5, and (ii) negatively interfering with the innate immune response against HAdV-5. More insight into the mechanisms by which the presence of protein IX affects gene transfer and activation of immune cells may be of use for enhancing the efficiency of current (e.g.³³) and future gene therapies involving protein IX modified HAdV-5 vectors.

MATERIALS AND METHODS

Cell lines

All cell lines were maintained as monolayers at 37°C in a humidified atmosphere of 5% CO₂. The human cell lines HeLa (cervical cancer), A549 (carcinomic alveolar epithelium), MEL2A (melanoma), MZ2-MEL3.0 (melanoma),⁵ VH10 (primary foreskin fibroblasts),³⁴ HepG2 (hepatocellular carcinoma), and 911 cells (HAdV-5 E1-transformed human embryonic retinoblasts)³⁵ were maintained in Dulbecco's Modified Eagle's Medium (DMEM) (Gibco-BRL, Breda, The Netherlands) supplemented with 8% fetal bovine serum (FBS) (Gibco-BRL, Breda, The Netherlands) and penicillin-streptomycin mixture.

Lentivirus transduction was used to create a MZ2-MEL3.0 cell line stably expressing human CAR. To this end, the CAR gene was PCR-amplified by using primers 1 and 2 (**Table 1**) from plasmid pCMV_hCAR (kindly provided by Dr. J.M. Bergelson¹⁴). The *Pst*I+*Nhe*I digested PCR product was ligated in between the corresponding restriction sites of pLV.CMV.IRES.PURO³⁶, resulting in pLV.CMV.CAR.IRES.PURO. The virus LV.CMV.CAR.IRES.PURO was produced by a previously described procedure involving cotransfection of pLV.CMV.CAR.IRES.PURO together with helper plasmids encoding HIV-1 gag-pol, HIV-1 rev, and the VSV-G envelope³⁷. The methods for determining the titer of the LV.CMV.CAR.IRES.PURO vector stock and the procedures for transduction of the MZ2-MEL3.0 cells have been described before³⁶. Selection for antibiotic resistance was achieved by seeding the cells in medium with 0.6 µg/ml puromycin (MP Biomedicals, Amsterdam, The Netherlands).

Viruses

The vectors HAdV-5.CMV.GFP/LUC¹² (Ad5ΔE1+pIX) and HAdV-5ΔpIX.CMV.GFP/LUC¹² (Ad5ΔE1ΔpIX) contain a green fluorescent protein (GFP) gene as well as a firefly luciferase (LUC) gene, which are both driven by a human cytomegalovirus (CMV) promoter. The vector HAdV-5pIXΔ100-114.CMV.LUC (Ad5ΔE1pIX^{ΔLEU}), encoding LUC

only, was described previously as well.⁴ Titration of the vector stocks was performed by a PicoGreen-DNA binding assay to determine the concentration in physical vector particles per ml (pp/ml).³⁸ A standard agar overlay plaque assay on 911 cells was used to determine the infectious virus concentration in plaque forming units per ml (pfu/ml).³⁵ The pp/pfu ratios of the three vectors were very similar, within the range of 10 to 12.

The replication-competent viruses HAdV-5.ΔE3.ADP.eGFP (Ad5+pIX) and HAdV-5.ΔE3.ADP.eGFP.ΔpIX (Ad5ΔpIX) were constructed by recombination of the shuttle plasmids pShuttle+E1+pIX (pSh+pIX) and pShuttle+E1ΔpIX (pShΔpIX) with a HAdV-5 backbone plasmid containing the eGFP gene in the E3 region (pBB). The plasmids pSh+pIX, pShΔpIX and pBB were constructed as follows. The wild-type HAdV-5 *BsrGI-MfeI* fragment containing the E1 genes (nucleotides 193-3925) was isolated from pTG3602 (kindly provided by Dr. M. Luski, Transgene, Strasbourg, France), and cloned into the *BsrGI-MfeI* digested pTrackCMV-GFP/LUC,¹² thereby replacing the GFP/LUC genes with the HAdV-5 E1 region. By using site-directed mutagenesis (QuikChange site-directed mutagenesis kit; Stratagene) (primers 3, 4, 5, 6 (**Table 1**)) two restriction sites were introduced in the protein IX gene; a *Scal* site at the start codon of protein IX and a *SpeI* site upstream of the protein IX stop codon, thereby creating pShuttle+E1+pIX^{Scal/SpeI}. Next, the pShΔpIX plasmid was constructed by *Scal/SpeI* digestion and re-ligation of the protein IX gene-deleted fragment. The pSh+pIX plasmid was created by introducing the protein IX sequence (amplified from pAd5pIX⁷ by using primers 7 and 8 (**Table 1**)) into the *Scal/SpeI* linearized pShuttleE1+pIX^{Scal/SpeI}. The *Scal*-site was restored to the wild-type HAdV-5 sequence by exchanging the *Scal*-overlapping *MfeI/HindIII* fragment with the corresponding fragment from pTG3602. The *SpeI* site and the downstream 'pIX-remainder sequence' were left intact, since part of this sequence forms a hairpin-loop structure situated over the polyA site of the E1B transcript, which might be essential for efficient polymerase slippage needed for polyadenylation.³⁹

The pBB backbone plasmid was constructed by replacing the E3-lacking *SpeI-PacI* fragment (nucleotides 27238-33443) of pAdEasy-1⁴⁰ with the corresponding *SpeI-PacI* fragment of pShuttle-ΔE3-ADP-EGFP-F2⁴¹, thereby introducing eGFP in the E3 region under control of the viral major late promoter. The coding sequence for the E3 Adenovirus Death Protein (ADP) was retained. The kanamycin resistance gene (inserted with the pShuttle-ΔE3-ADP-EGFP-F2 fragment) was removed by *Clal* digestion and re-ligation of the two largest fragments.

Recombination of pBB with pSh+pIX and pShΔpIX in *E.coli* and subsequent virus rescue in A549 cells were performed as described elsewhere.⁴⁰ Virus was purified by a standard double cesium chloride gradient protocol, dialyzed against sucrose buffer (5% sucrose, 140 mM NaCl, 5 mM Na₂HPO₄·2H₂O, 1.5 mM KH₂PO₄) and stored at -80°C. The virus titer was determined by the PicoGreen-DNA binding assay³⁸ (for pp/ml measurement), and a plaque assay on A549 cells³⁵ (for pfu/ml measurement). For analysis of virus spread, GFP positive plaques were photographed (Olympus Camedia Digital Camera C-3030, installed on an Olympus CK40 microscope) and the plaque size was determined in arbitrary units (Olympus DP-soft v.5.0 Soft imaging System software). The median plaque size of Ad5ΔpIX was normalized to the plaque size for Ad5+pIX.

Table 1. Oligonucleotides used in the cloning procedures.

FWD CAR_PstI	5'-GATGTA CTGCAGATGGCGCTCCTGCTGTG-3'
REV CAR NheI	5'-CGACGCTAGCTATACTATAGACCCATCCTTGCTCTG-3'
FWD Scal_correct	5'-TTGCAGCAGCCGCCGCCAGTACTAGCACCAACTCGTTTGATGG-3'
REV Scal_correct	5'-CCATCAAACGAGTTGGTGCTAGTACTGGCGGCGGCGGCTGCTGCAA-3'
FWD SpeI_correct	5'-GGTTTCTGCCCTGAAGGCTTACTAGTCTCCCAATGCGGTTTAAAC-3'
REV SpeI_correct	5'-GTTTTAAACCGCATTGGGAGACTAGTAAGCCTTCAGGGCAGAAACC-3'
FWD pIX_Scal	5'-CGCGGAAGTACTATGAGCACCAACTCGTTTGATGG-3'
REV pIX_SpeI	5'-CGCACTAGTTTAAACCGCATTGGGAGGGGAGG-3'

Analysis of CAR presentation on the cell surface

Flow cytometry was performed to determine the levels of CAR presentation on the cell surface. Cells in suspension (in PBS with 0.5% bovine serum albumin and 0.02% sodium azide) were incubated with mouse monoclonal anti-CAR antibody (clone RmCB, Upstate Biotechnology, Lake Placid, NY, diluted 1:1000) for 30 min on ice, followed by incubation with phycoerythrin (PE)-conjugated rabbit-anti-mouse secondary antibody (Caltac Laboratories, Burlingame, CA, USA) for 30 min on ice. Flow cytometry data were analyzed with CellQuest software (Becton Dickinson).

Immunohistochemistry was performed on the cell line MZ2-MEL3.0/CAR. After washing with phosphate-buffered saline (PBS), the cells were fixed in acetone/methanol (1:1) for 10 min at room temperature. Staining was performed with the anti-CAR antibody (clone RmCB, Upstate Biotechnology, Lake Placid, NY, diluted 1:500). Fluorescein isothiocyanate (FITC)-conjugated rabbit-anti-mouse antibody (Jackson ImmunoResearch, France) was used as secondary antibody.

Virus transduction assays

(1) Luciferase expression

The transduction efficiency of CAR-positive (HeLa, A549, MEL2A, MZ2-MEL3.0/CAR) and CAR-negative (MZ2-MEL3.0, VH10) cell lines by Ad5ΔE1+pIX and Ad5ΔE1ΔpIX was compared by measuring luciferase expression. Transduction was performed in triplicate in 24-well plate wells in 500 μl DMEM/8% FBS. After a two-hours incubation the virus-containing medium was replaced with fresh medium without virus. At 24 hours post transduction the cells were washed once with PBS and lysed in 100 μl LUC-lysis mix (25 mM Tris-phosphate (pH 7.8), 2 mM CDTA, 2 mM DTT, 10% glycerol and 1% Triton-X in PBS). Luciferase production was determined with the Promega Luciferase Assay by adding 25 μl luciferase assay reagent to 10 μl lysate. Light intensity measurement was performed in a Victor Wallac 2 microplate reader (PerkinElmer, Inc., Waltham, MA, USA).

(2) Integrin blocking

Indirect blocking of integrin-mediated virus uptake was performed by incubating cells with EDTA. MZ2-MEL3.0 cells were harvested from semi-confluent tissue culture plates, washed three times in PBS with 5 mM EDTA, and resuspended in standard PBS

or PBS supplemented with 0.9 mM CaCl₂ and 0.5 mM MgCl₂ (PBS⁺⁺). The Ad5ΔE1+pIX and Ad5ΔE1ΔpIX stocks were adjusted to equal pp concentrations by adding sucrose buffer and were diluted 1:1 in a 5 mM EDTA solution in PBS. Virus (100 pp/cell) was added to 500,000 cells in 1 ml PBS or PBS⁺⁺ and incubation was performed for 60 min at 37°C under constant agitation. Subsequently, the cells were pelleted by centrifugation, dissolved in 5 ml medium and transferred to 24-well plate wells (500 μl per well). Cells were incubated for 24 hours and analyzed for GFP expression by flow cytometry. Data were analyzed with CellQuest software (Becton Dickinson).

The anti-human CD51/61 monoclonal antibody (MAb LM609), an αVβ3 integrin antagonist, and MAb P1F6, an αVβ5 integrin antagonist (both obtained from Millipore) were used to test the inhibitory effect of anti-integrin antibodies on virus transduction. Cells grown as monolayers were pre-incubated with medium only or with medium containing integrin function-blocking MAbs (10 mg/ml). After 30 min of incubation, the excess antibody was removed by gentle washing followed by virus transduction (100 pp/cell). Reporter gene expression was measured 24 hours post transduction by performing a standard luciferase assay.

(3) *Virus incubation with coagulation factor X (FX)*

HepG2 and A549 cells were plated in 24-well plate wells. After a PBS wash step, Ad5ΔE1+pIX or Ad5ΔE1ΔpIX (100 pp/cell) was added in serum-free medium containing 8 μg/ml Factor X (FX) (HCX-0050, Haemotologic Technologies Inc.), 8 μg/ml Gla-domainless Factor X (FX^{MUT}) (HCX-GD, Haemotologic Technologies Inc.) or no FX/FX^{MUT}. After 2 hours the medium was replaced by normal medium. Luciferase expression was measured 24 hours post transduction.

Immunoblot analysis and electron microscopy

Immunoblot analyses were performed to assess the incorporation of proteins into the capsid of Ad5ΔE1+pIX and Ad5ΔE1ΔpIX. The western blotting and detection procedures were described previously.⁵ Virus lysates were prepared by adding 5×10⁹ virus particles directly to western sample buffer. Capsid proteins were visualized with rabbit polyclonal anti-protein IX serum (1:2000,⁴² goat polyclonal anti-hexon (1:1000, ab19998, Abcam, Cambridge, UK), and mouse monoclonal anti-fiber (1:5000, 4D2, Abcam).⁴³ Secondary antibodies were horseradish peroxidase (HRP)-conjugated goat-anti-rabbit and rabbit-anti-mouse (Santa Cruz Biotechnology, Inc., Santa Cruz, CA, USA).

Electron microscopy was performed on Ad5ΔE1+pIX and Ad5ΔE1ΔpIX samples adsorbed into glow-discharged carbon coated copper grids and negatively stained for 30 seconds with 2% phosphotungstic acid (pH 7). The viruses were examined with a FEI Tecnai Spirit BioTwin transmission electron microscope operating at 120 kV. Images were recorded on a 4k × 4k Eagle CCD camera.

PBMC analysis

Buffy coats were obtained from healthy donors after consent (Sanquin Bloodbank, Leiden, The Netherlands) and centrifuged on a Ficoll gradient to obtain PBMC. PBMC (1 × 10⁶) were added to a well of a 24-well plate in 0.5 ml medium (RPMI/10%FCS) and virus was added at the indicated MOI in 0.5 ml medium. After incubation at 37°C and 5% CO₂ for two days, the supernatants were isolated for interferon gamma (IFN-γ) measurement, and the cells were prepared for flow cytometry analysis. Cells were

washed twice with PBS/0.02% sodium azide, fixed for 10 min in 4% paraformaldehyde, washed twice with PBS/0.5% BSA/0.02 sodium azide, and stained with antibodies. Antibodies used were anti-CD3-PerCP-Cy5.5, anti-CD4-PE, anti-CD14-APC, anti-CD14-PerCP-Cy5.5, anti-CD19-PE, anti-CD19-PerCP-Cy5.5, anti-CD69-PE and anti-CD86-PE (Becton Dickinson, Franklin Lakes, NJ, USA), anti-CD8-APC and anti-CD56-APC (Beckman Coulter, Brea, CA, USA). Activation of NK cells was evaluated as increased CD69 expression on CD3-, CD14-, CD19-, CD56+ cells. Monocyte activation was analyzed as increased CD86 expression on CD3-, CD19-, CD14+ cells. Fluorescence was measured by flow cytometry on a FACS Calibur (Becton Dickinson) and data were analyzed with CellQuest software (Becton Dickinson). IFN- γ in supernatants was measured by ELISA using the PeliPair reagent set for human IFN- γ (Sanquin, Amsterdam, NL).

Viral distribution after intravenous delivery

Ad5 Δ E1+pIX or Ad5 Δ E1 Δ pIX (10^9 pp) was injected in the tail vein of 6-week-old athymic nude mice (NMRI nu/nu; Taconic M&B A/S, Ry, Denmark), followed by sacrificing the animals and harvesting of multiple organs at 3 days post injection. Four hours before Ad5 Δ E1+pIX and Ad5 Δ E1 Δ pIX injection, pre-dosing was performed with the empty vector HAdV-5.CMV (replication-deficient and not encoding a transgene) (5×10^{10} pp) to saturate Kupffer cell macrophages. Tissue samples from each organ were lysed in LUC-lysis mix and the luciferase expression was measured according to the Promega Luciferase Assay. The protein concentration in the lysates was determined by using the bicinchoninic acid protein assay (Pierce, Perbio Science BV, Etten-Leur, The Netherlands), enabling the calculation of luciferase expression per total protein. The experiment was performed under the Dutch Experiments on Animals Act that serves the implementation of "Guidelines on the protection of experimental animals" by the Council of Europe (1986), Directive 86/609/EC, and only after a positive recommendation by the Animal Experiments Committee.

ACKNOWLEDGEMENTS

We thank Jort Vellinga and Vivien Mautner for valuable scientific discussions and critically reading the manuscript, Steve Cramer for expert technical support, and Martijn Rabelink for producing the viruses used in these studies. This work was supported by the European Union through the 6th Framework Program GIANT (contract no. 512087).

REFERENCES

1. Vellinga J, Van der Heijdt S, Hoeben RC. The adenovirus capsid: major progress in minor proteins. *J Gen Virol* 2005; **86**: 1581-1588.
2. Fabry CMS, Rosa-Calatrava M, Moriscot C, Ruigrok RWH, Boulanger P, Schoehn G. The C-terminal domains of adenovirus serotype 5 protein IX assemble into an antiparallel structure on the facets of the capsid. *J Virol* 2009; **83**: 1135-1139.
3. Saban SD, Silvestry M, Nemerow GR, Stewart PL. Visualization of alpha-helices in a 6-angstrom resolution cryoelectron microscopy structure of adenovirus allows refinement of capsid protein assignments. *J Virol* 2006; **80**: 12049-12059.
4. Vellinga J, van den Wollenberg DJM, van der Heijdt S, Rabelink MJWE, Hoeben RC. The coiled-coil domain of the adenovirus type 5 protein IX is dispensable for capsid incorporation and thermostability. *J Virol* 2005; **79**: 3206-3210.
5. de Vrij J, Uil TG, van den Hengel SK, Cramer SJ, Koppers-Lalic D, Verweij MC et al. Adenovirus targeting to HLA-A1/MAGE-A1-positive tumor cells by fusing a single-chain T-cell receptor with minor capsid protein IX. *Gene Ther* 2008; **15**: 978-989.
6. Vellinga J, de Vrij J, Myhre S, Uil T, Martineau P, Lindholm L et al. Efficient incorporation of a functional hyperstable single-chain antibody fragment protein-IX fusion in the adenovirus capsid. *Gene Ther* 2007; **14**: 664-670.
7. Vellinga J, Rabelink MJWE, Cramer SJ, van den Wollenberg DJM, Van der Meulen H, Leppard KN et al. Spacers increase the accessibility of peptide ligands linked to the carboxyl terminus of adenovirus minor capsid protein IX. *J Virol* 2004; **78**: 3470-3479.
8. Corjon S, Wortmann A, Engler T, van Rooijen N, Kochanek S, Kreppel F. Targeting of adenovirus vectors to the LRP receptor family with the high-affinity ligand RAP via combined genetic and chemical modification of the pIX capsomere. *Mol Ther* 2008; **16**: 1813-1824.
9. Tang Y, Wu H, Ugai H, Matthews QL, Curiel DT. Derivation of a triple mosaic adenovirus for cancer gene therapy. *PLoS One* 2009; **4**: e8526.
10. Bayer W, Tenbusch M, Lietz R, Johrden L, Schimmer S, Uberla K et al. Vaccination with an adenoviral vector that encodes and displays a retroviral antigen induces improved neutralizing antibody and CD4+ T-cell responses and confers enhanced protection. *J Virol* 2010; **84**: 1967-1976.
11. Boyer J, Sofer-Podesta C, Ang J, Hackett N, Chiuchiolo M, Senina S et al. Protective Immunity Against a Lethal Respiratory Yersinia pestis Challenge Induced by V Antigen or the F1 Capsular Antigen Incorporated into the Adenovirus Capsid. *Hum Gene Ther* 2010; **21**: 891-901.
12. Vellinga J, Uil TG, de Vrij J, Rabelink MJWE, Lindholm L, Hoeben RC. A system for efficient generation of adenovirus protein IX-producing helper cell lines. *J Gene Med* 2006; **8**: 147-154.
13. Fabry CM, Rosa-Calatrava M, Conway JF, Zubieta C, Cusack S, Ruigrok RW et al. A quasi-atomic model of human adenovirus type 5 capsid. *EMBO J* 2005; **24**: 1645-1654.
14. Bergelson JM, Cunningham JA, Droguett G, Kurt-Jones EA, Krithivas A, Hong JS et al. Isolation of a common receptor for Coxsackie B viruses and adenoviruses 2 and 5. *Science (New York, NY)* 1997; **275**: 1320-1323.
15. Nemerow GR, Stewart PL. Role of alpha(v) integrins in adenovirus cell entry and gene delivery. *Microbiol Mol Biol Rev* 1999; **63**: 725-734.
16. Wickham TJ, Mathias P, Cheresch DA, Nemerow GR. Integrins alpha v beta 3 and alpha v beta 5 promote adenovirus internalization but not virus attachment. *Cell* 1993; **73**: 309-319.
17. de Haan CA, Li Z, te Lintelo E, Bosch BJ, Haijema BJ, Rottier PJ. Murine coronavirus with an extended host range uses heparan sulfate as an entry receptor. *J Virol* 2005; **79**: 14451-14456.
18. Kalyuzhnyi O, Di Paolo NC, Silvestry M, Hoffherr SE, Barry MA, Stewart PL et al. Adenovirus serotype 5 hexon is critical for virus infection of hepatocytes *in vivo*. *Proc Natl Acad Sci USA* 2008; **105**: 5483-5488.

19. Waddington SN, McVey JH, Bhella D, Parker AL, Barker K, Atoda H et al. Adenovirus serotype 5 hexon mediates liver gene transfer. *Cell* 2008; **132**: 397-409.
20. Patterson S, Russell WC. Ultrastructural and immunofluorescence studies of early events in adenovirus-HeLa cell interactions. *J Gen Virol* 1983; **64**: 1091-1099.
21. Reiser H, Stadecker MJ. Costimulatory B7 molecules in the pathogenesis of infectious and autoimmune diseases. *N Engl J Med* 1996; **335**: 1369-1377.
22. McNees AL, Mahr JA, Ornelles D, Gooding LR. Postinternalization inhibition of adenovirus gene expression and infectious virus production in human T-cell lines. *J Virol* 2004; **78**: 6955-6966.
23. Drouin M, Cayer MP, Jung D. Adenovirus 5 and chimeric adenovirus 5/F35 employ distinct B-lymphocyte intracellular trafficking routes that are independent of their cognate cell surface receptor. *Virology* 2010; **401**: 305-313.
24. Heemskerk B, Veltrop-Duits LA, van Vreeswijk T, ten Dam MM, Heidt S, Toes RE et al. Extensive cross-reactivity of CD4+ adenovirus-specific T cells: implications for immunotherapy and gene therapy. *J Virol* 2003; **77**: 6562-6566.
25. Cambiaggi C, Scupoli MT, Cestari T, Gerosa F, Carra G, Tridente G et al. Constitutive expression of CD69 in interspecies T-cell hybrids and locus assignment to human chromosome 12. *Immunogenetics* 1992; **36**: 117-120.
26. Trinchieri G, Matsumoto-Kobayashi M, Clark SC, Seehra J, London L, Perussia B. Response of resting human peripheral blood natural killer cells to interleukin 2. *J Exp Med* 1984; **160**: 1147-1169.
27. He XS, Draghi M, Mahmood K, Holmes TH, Kemble GW, Dekker CL et al. T cell-dependent production of IFN-gamma by NK cells in response to influenza A virus. *J Clin Invest* 2004; **114**: 1812-1819.
28. Muruve DA. The innate immune response to adenovirus vectors. *Hum Gene Ther* 2004; **15**: 1157-1166.
29. Di Paolo NC, Shayakhmetov DM. Adenovirus de-targeting from the liver. *Curr Opin Mol Ther* 2009; **11**: 523-531.
30. Xu Z, Tian J, Smith JS, Byrnes AP. Clearance of adenovirus by Kupffer cells is mediated by scavenger receptors, natural antibodies, and complement. *J Virol* 2008; **82**: 11705-11713.
31. Au T, Thorne S, Korn WM, Sze D, Kirn D, Reid TR. Minimal hepatic toxicity of Onyx-015: spatial restriction of coxsackie-adenoviral receptor in normal liver. *Cancer Gene Ther* 2007; **14**: 139-150.
32. Bangari DS, Shukla S, Mittal SK. Comparative transduction efficiencies of human and nonhuman adenoviral vectors in human, murine, bovine, and porcine cells in culture. *Biochem Biophys Res Commun* 2005; **327**: 960-966.
33. Atencio IA, Grace M, Bordens R, Fritz M, Horowitz JA, Hutchins B et al. Biological activities of a recombinant adenovirus p53 (SCH 58500) administered by hepatic arterial infusion in a Phase 1 colorectal cancer trial. *Cancer Gene Ther* 2006; **13**: 169-181.
34. Klein B, Pastink A, Odijk H, Westerveld A, van der Eb AJ. Transformation and immortalization of diploid xeroderma pigmentosum fibroblasts. *Exp Cell Res* 1990; **191**: 256-262.
35. Fallaux FJ, Kranenburg O, Cramer SJ, Houweling A, Van Ormondt H, Hoeben RC et al. Characterization of 911: a new helper cell line for the titration and propagation of early region 1-deleted adenoviral vectors. *Hum Gene Ther* 1996; **7**: 215-222.
36. Uil TG, de Vrij J, Vellinga J, Rabelink MJWE, Cramer SJ, Chan OYA et al. A lentiviral vector-based adenovirus fiber-pseudotyping approach for expedited functional assessment of candidate retargeted fibers. *J Gene Med* 2009; **11**: 990-1004.
37. Carlotti F, Bazuine M, Kekarainen T, Seppen J, Pognonec P, Maassen JA et al. Lentiviral vectors efficiently transduce quiescent mature 3T3-L1 adipocytes. *Mol Ther* 2004; **9**: 209-217.
38. Murakami P, McCaman MT. Quantitation of adenovirus DNA and virus particles with the PicoGreen fluorescent Dye. *Anal Biochem* 1999; **274**: 283-288.
39. Sittler A, Gallinaro H, Jacob M. The secondary structure of the adenovirus-2 L4 polyadenylation domain: evidence for a hairpin structure exposing the

- AAUAAA signal in its loop. *J Mol Biol* 1995; **248**: 525-540.
40. He TC, Zhou S, da Costa LT, Yu J, Kinzler KW, Vogelstein B. A simplified system for generating recombinant adenoviruses. *Proc Natl Acad Sci USA* 1998; **95**: 2509-2514.
 41. Ono HA, Le LP, Davydova JG, Gavrikova T, Yamamoto M. Noninvasive visualization of adenovirus replication with a fluorescent reporter in the E3 region. *Cancer Res* 2005; **65**: 10154-10158.
 42. Caravokyri C, Leppard KN. Constitutive episomal expression of polypeptide IX (pIX) in a 293-based cell line complements the deficiency of pIX mutant adenovirus type 5. *J Virol* 1995; **69**: 6627-6633.
 43. Hong JS, Engler JA. The amino terminus of the adenovirus fiber protein encodes the nuclear localization signal. *Virology* 1991; **185**: 758-767.

